Report no. changed (Mar 2006): SM-293-UU

SACLANTCEN MEMORANDUM
serial no.: SM-293

SACLANT UNDERSEA
RESEARCH CENTRE
MEMORANDUM

DETECTION OF OBJECTS ON A NON RAYLEIGH BACKGROUND

B. Stage

December 1995

SACLANT Undersea Research Centre
Viale San Bartolomeo 400
19138 San Bartolomeo (SP), Italy

tel: +39-187-540.111
fax: +39-187-524.600

e-mail: library@saclantc.nato.int

NORTH ATLANTIC TREATY ORGANIZATION

Detection of objects on a non Rayleigh background

B. Stage

The content of this document pertains to work performed under Project 25 of the SACLANTCEN Programme of Work. The document has been approved for release by The Director, SACLANTCEN.

Director

Detection of objects on a non Rayleigh background

B. Stage

Executive Summary: Sea–bottom scattering often makes it difficult for the mine hunting sonar operator to distinguish an object from the background. This report describes a novel approach to processing information from sea–bottom scatterers. It is shown that by considering the statistical information from sea–bottom objects, as the sonar viewing angle changes, it is possible to gain additional classification clues for potential targets. For the operator it means that the ability to discriminate between objects and background will improve. The technique can be used for long range classification.

Detection of objects on a non Rayleigh background

B. Stage

Abstract: Sector scanning sonar systems image the sea–bottom to detect objects that can be distinguished from the background structure of the sea–bottom. In current systems images are displayed and discarded as new image data become available. In this report a method for improving sonar detection by utilizing all images in a sequence is investigated. The proposed method requires that sonar data are acquired with a sector scanning sonar in a side–looking configuration. It is demonstrated that these data can be used to detect observation point dependent changes in sea-bottom backscattering characteristics. These changes provide additional cues for discrimination that can improve the detection of objects on the sea–bottom. Results of applying the method to experimental data are presented. Keywords: Detection, Observation point, Backscattering.

Contents

1
Introduction

Sector scanning sonar systems are used to image the sea-bottom in order to detect man made objects that can be distinguished from the background structure of the sea-bottom. Object detection is performed by an operator examining a real time image of the acoustic backscattering properties of the sea–bottom scene. The objects of interest are assumed to have higher backscattering than the sea bottom background and the presence of an object is declared when the image amplitude observed at a location significantly exceeds the amplitude of the background. The detection efficiency is limited by the average image amplitude level of the background as well as temporal and spatial fluctuations in image amplitude characteristic of coherent imaging systems.

The classical model used to describe the amplitude fluctuations assumes the bottom background signal to arise from the sum of signals returned from a large number of point scatterers of comparable scattering amplitude, uniformly distributed on the bottom surface [1]–[3]. According to this model the spatial variation in the image amplitude of the background is described as a Rayleigh distributed random field.

Spatial variation in image amplitude that deviates from the Rayleigh distribution has been reported [4]–[8]. The deviations reported are in many cases such that the probability of obtaining a large amplitude value is higher than predicted by the Rayleigh distribution. This type of data has been described by first order empirical distributions such as exponential, Weibull, chi-square, log-normal, Rice and K [7], [9]. Detection of objects on a non Rayleigh distributed background has been studied in radar [10]. If the amplitude of the background has a probability density function with thicker tails than the Rayleigh, the detection threshold must be raised to avoid an unacceptably high false alarm probability and the decreased detection performance has to be accepted.

As an alternative to raising the detection threshold, more information on the bottom characteristics could be acquired to allow discrimination between normal background and objects of interest. Instead of basing the discrimination on the amplitude in a single image it is suggested that the discrimination be based on a sequence of images, acquired while moving the sonar over an area of sea bottom.

The outline of the report is as follows. First a model of the signal received from a point on the bottom is described with emphasis on the variation in the received signal with the position of the sonar i.e grazing angle, bearing angle and range. The variation in the received signal with bearing angle is investigated by simulations and it is suggested to measure this variation by means of a side looking sector scanning sonar. A method to discriminate between parts of the sea bottom with different variation in the received signal as a function of bearing angle is suggested and experimental data is used to demonstrate the utility of the method.

2
Signal characteristics

A sonar image of the sea–bottom is constituted from samples of the backscattered signal from the sea–bottom scene. This section discusses the characteristics of these samples and the extent to which it is possible to measure the backscattering properties independently of the measuring system.

Consider the experimental situation shown in Fig. 1. A sample is measured by interrogating the sea bottom around a position (x, y) with a narrow band pulse-echo sonar system at low grazing angles. The position is determined in a coordinate system fixed to the bottom with the xy plane on the mean plane of the bottom which is assumed to be flat. The position of the sonar aperture is determined by the slant range r, the grazing angle θ with respect to the xy plane and the bearing angle ψ with respect to the xz plane.

The signal received by the sonar from a position (x, y) on the bottom originates from scattering structures located within an area corresponding to the resolution cell of the sonar system. In the farfield of the sonar aperture the resolution cell on the sea–bottom is approximately rectangular. The range resolution Δl is

$$\Delta l = \frac{c\tau_p}{2\cos\theta} , \tag{1}$$

where c is the speed of sound in the medium and τ_p is the duration of the interrogating pulse, possibly after pulse compression filtering. In the farfield of the sonar aperture the bearing resolution Δw is

$$\Delta w = a_w \frac{\lambda}{D} r , \tag{2}$$

where λ is the wavelength of the ensonification, D is the size of the aperture, and a_w is a constant determined by the aperture shading and the choice of beamwidth criterion.

The received signal will depend on both the scattering structures within the resolution cell and the relative position of the sonar. Assuming that only bottom backscattering contributes to the received signal and that the propagation medium is stable and non dispersive the received narrow band signal represented in terms of its complex envelope $\tilde{s}(x, y, r, \theta, \psi)$ can be expressed as

$$\tilde{s}(x, y, r, \theta, \psi) = \Upsilon(r, \theta)\, \tilde{b}(x, y, r, \theta, \psi) \tag{3}$$

The amplitude response function $\Upsilon(r,\theta)$ describes the variation in received signal amplitude as a function of the position of the resolution cell relative to the sonar. This variation is due to two way aperture directivity and transmission loss. The backscattering from the structures within the resolution cell is described by the complex backscattering function $\tilde{b}(x,y,r,\theta,\psi)$. A qualitative understanding of the interaction process can be gained by considering an assembly of point scatterers, each returning a scaled replica of the incoming pulse. The backscattering function can then be expressed as the coherent sum of the scattering amplitudes of the scatterers within the resolution cell. Letting m be the number of scatterers within the area bounded by Δl and Δw, the backscattering function is given by

$$\tilde{b}(x,y,r,\theta,\psi) = \sum_m b_m \exp(i\frac{4\pi}{\lambda}r_m) , \tag{4}$$

where b_m is the scattering amplitude of the mth scatterer located at a distance r_m from the sonar aperture.

The normalized envelope amplitude $a(x,y,r,\theta,\psi)$ is defined as the envelope of the received signal normalized with respect to the amplitude response function and the ensonified area

$$a(x,y,r,\theta,\psi) = \frac{|\tilde{s}(x,y,r,\theta,\psi)|}{\Upsilon(r,\theta)\sqrt{\Delta w \Delta l}} . \tag{5}$$

The samples of the normalized envelope amplitude describe a property of a point on the sea bottom independent, to the extent possible, of the measuring system and the propagation medium. The remaining system dependence is due to the change in orientation and size of the resolution cell.

By defining a point on the sea–bottom as the centre of the resolution cell of a sonar system, the preceeding discussion has shown that the signal received from this point will depend on the position of the sonar system. The normalized envelope amplitude measured from this point will vary as the width of the resolution cell changes with range, the length of the resolution cell changes with grazing angle and the orientation of the resolution cell changes with bearing angle.

3

Signal variation with sonar position

An important characteristic of the envelope amplitude is the sensitivity to changes in range, grazing angle and bearing angle. The sensitivity can be characterized by considering the change necessary to produce independent samples.

The main effect resulting from a change in range is the change in the width Δw of the resolution cell as seen from Eq. 2. When the width of the resolution cell is changed, scatterers on the sea–bottom bordering the resolution cell are added or removed. This will cause a change in the measured value of the sample. However, as the scatterers at the centre of the resolution cell and their relative distances to the aperture remain unchanged, samples acquired with resolution cells of different width, but centered at the same point on the sea–bottom, will be correlated. The correlation between two samples acquired at different ranges will decrease as the difference of the ranges increases, but will remain finite.

An independent sample can be acquired by changing the bearing or grazing angle in order that the two way path length to the sonar changes by more than half a wavelength for the dominant scatterers within the resolution cell. As the positions of the scatterers are unknown it is required that the average two–way path length change within the resolution cell is half a wavelength. This is equivalent to requiring the two–way path length difference between the outermost positions in the resolution cell to be one wavelength.

By adopting this criterion the following condition is found for the change in bearing angle $\Delta\psi$:

$$2\ \Delta w\ [\sin(\psi + \Delta\psi) - \sin(\psi)] > \lambda \tag{6}$$

Using the small angle approximation $\sin\psi \approx \psi$ and substituting Δw from (2)

$$\Delta\psi > \frac{1}{2a_w}\frac{D}{r}\ . \tag{7}$$

This condition is equivalent to the requirement that the sonar aperture is translated $D/(2a_w)$ to obtain an independent measurement. Typically, the value of $D/(2a_w)$ for a detection sonar is from a quarter to half a meter.

The condition found for the change in grazing angle $\Delta\theta$ is:

$$2\ \Delta l\ [\cos(\theta) - \cos(\theta + \Delta\theta)] > \lambda\ . \tag{8}$$

Inserting Δl from Eq. 1 gives

$$\Delta\theta > \cos^{-1}[(1 - \frac{\lambda}{c\tau_p})\cos\theta] - \theta \ . \tag{9}$$

Typically, $\lambda/(c\tau_p)$ will be around 0.1. Thus, for zero grazing angle the required increment in grazing angle to obtain an independent sample is $\Delta\theta = 11.2°$. Therefore, only a few independent samples can be obtained by changing the grazing angle.

The above discussion is a qualitative indication that only small changes in bearing angle are required to obtain independent samples of the envelope amplitude whereas large changes in range and grazing angle are required to obtain the same result. The characteristics of the local backscattering function can thus be obtained by studying the variation of the normalized envelope amplitude with bearing angle independent of range and grazing angle within comparatively wide intervals.

4

Signal variation with bearing angle

The variation of the normalized envelope with bearing angle depends on the position and scattering amplitude of the structures within the resolution cell. No generally valid assumptions can be made regarding the bottom structures but some insight in the behaviour of the envelope amplitude can be gained by considering a few examples using the point scatterer model.

In the simplest case the sea bottom is flat and the bottom backscattering function is well described as the sum of the contributions from a large number of scatterers uniformly distributed on a plane. With known scatterer positions and amplitudes the backscattering function can be determined from Eq. 4 and the normalized envelope from Eq. 5.

Consider as an example 120 point scatterers distributed uniformly inside a rectangular region of 80 by 8 wavelength, as shown in Fig. 2a. The scattering amplitudes are uniformly distributed and the amplitude response function is unity. The variation of the envelope amplitude with bearing angle measured with respect to the x axis within an interval of 90° is shown in Fig. 2b. The range of fluctuation of the envelope amplitude is independent of bearing angle. The histogram of envelope amplitudes in Fig. 2c appears smooth and unimodal. The angular correlation of the envelope amplitude as determined from the autocovariance in Fig. 2d is in qualitative agreement with the condition in Eq. 6. The above example is well described by the classical first order statistical model where the backscattering function is assumed to be a stationary circular complex zero mean Gaussian process with variance σ_b^2. The envelope amplitude A is then described by the Rayleigh probability density function [11].

$$p(A) = \frac{A}{\sigma_b^2} \exp\left(-\frac{A^2}{2\sigma_b^2}\right) \tag{10}$$

The process is described by a single parameter σ_b. The mean value is $\sqrt{\frac{1}{2}\pi}\ \sigma_b$ and the variance is $(2 - \frac{1}{2}\pi)\ \sigma_b^2$.

As a second example, consider the signals returned from a strongly scattering smooth compact object on a flat bottom. This situation is modelled by introducing one strong point scatterer at the center of the background scatterers considered previously as illustrated in Fig. 3a. The scattering amplitude of the strong scatterer is

100 times larger than the average scattering amplitude of the background scatterers. The variation of envelope amplitude with bearing angle shown in Fig. 3b can also in this case be described as a stationary random process. The histogram of envelope amplitudes in Fig. 3c is smooth and unimodal, and the width of the autocovariance function in Fig. 3d is comparable to the width of the autocovariance function for the Rayleigh case in Fig. 2d. The backscattering function is the sum of a a stationary circular complex zero mean Gaussian process with variance σ_b^2 and a signal of constant phase with amplitude b. The samples of the envelope amplitude follow a Rice distribution [11] with a probability density function given by

$$p(A) = \frac{A}{\sigma_b^2} \exp\left(-\frac{A^2+b^2}{2\sigma_b^2}\right) I_0\left(\frac{Ab}{\sigma_b^2}\right) , \tag{11}$$

where $I_0(\cdot)$ is the modified Bessel function of order zero. When the amplitude of the constant signal is much smaller than the standard deviation of the random component $b \ll \sigma_b$ the Rice distribution converges to the Rayleigh distribution. At the other extreme when the amplitude of the constant signal is much greater than the standard deviation of the random component $b \gg \sigma_b$ the large argument approximation [12] $I_o(q) \approx (2\pi q)^{-1/2} \exp q$ gives

$$p(A) = \frac{1}{\sqrt{2\pi}\sigma_b}\sqrt{\frac{A}{b}} \exp\left(-\frac{(A-b)^2}{2\sigma_b^2}\right) . \tag{12}$$

In this case the probability density function is approximately Gaussian distributed with mean b and variance σ_b^2. The Rice process is completely described by two parameters.

Consider next the signal returned from an object with two strong scattering centers on a flat bottom. In Fig. 4a the position of the point scatterers considered previously are shown with two strong point scatterer of equal amplitude 4 wavelengths apart. The scattering amplitudes of the strong point scatterers are equal and 50 times larger than the average scattering amplitude of background scatterers. In addition to random uncorrelated fluctuations the envelope amplitude shown in Fig. 4b exhibits a periodic variation with bearing angle. This blinking is caused by interference between the two dominant scatterers. Compared to the examples considered previously, the histogram of envelope amplitudes in Fig. 4c shows a larger relative spread and the mode is displaced towards higher values. The autocovariance function in Fig. 4d is wider than that of the previous examples. The variation of the envelope amplitude can be characterized by three parameters: the amplitude of the periodic variation, the frequency of the variation and the standard deviation of the background. The process is not described completely by a first order probability density function as this would contain no information on the angular correlation. Further complexity could be added by introducing unequal scattering amplitudes and more dominant scatterers. The probability density functions for these cases can be determined numerically [13]. The inverse problem of estimating the parameters of the generating process from a limited number of noisy samples of the envelope amplitude becomes difficult even for a small number of dominant point scatterers. In the limit where the number of strong scatterers becomes large and no single scatterer is dominant the process will converge to the Rayleigh process.

In the above examples the positions of the scattering structures was assumed to be random. In practice the features of the sea bottom will exhibit some spatial ordering such as objects with facets larger than the wavelength or ripples on the sea bottom. A simple form of spatial ordering is scatterers randomly distributed on a segment of a straight line. The positions of the point scatterers considered previously are shown in Fig. 5a. In addition 120 point scatterers are distributed uniformly on a line segment. The backscattering amplitude distribution of the scatterers on the line is identical to that of the background scatterers. The envelope amplitude variation with bearing angle in Fig. 5b resembles the Rayleigh process except for an interval with a glint where the sonar line of sight is perpendicular to the line of scatterers. The histogram of envelope amplitudes shown in Fig. 5c resembles a Rayleigh probability density function except for some high values due to the glint. The autocovariance function in Fig. 5d is wider than in the case of a Rayleigh process. The variation of the envelope amplitude can be characterized by four parameters: the glint amplitude, the glint width, the angular position and the standard deviation of the background. The process is non stationary and cannot be completely described by a first order statistical model.

The general variation of the envelope amplitude with bearing angle can be expected to be at least as complicated as any combination of the above examples. The process can be expected to be non stationary and the samples can be expected to be correlated. A complete description of the process will require a large number of parameters. A first order statistical model will not be a complete description.

The spatial variation of the envelope amplitude for a fixed position of the sonar can be understood by considering a resolution cell with a behaviour as discussed above to be associated with each independent spatial position. A complete description of the spatial variation will thus require the specification of a process and associated process parameters at each spatial position.

5

Noise

Experiments indicate that variation in the envelope amplitude of signals received from the sea–bottom for a fixed sonar position is non negligible [14]. The variation can be caused by ambient noise, volume scattering from moving scatterers and instabilities in the medium.

When volume scattering and ambient noise can be considered the sum of many independent events of comparable significance an adequate model is a circular complex zero mean Gaussian process $\tilde{n}(r)$ with range dependent variance. The received signal can then be expressed as

$$\tilde{s}(x, y, r, \theta, \psi) = \Upsilon(r, \theta)\, \tilde{b}(x, y, r, \theta, \psi) + \tilde{n}(r)\ . \tag{13}$$

Measurements of the envelope amplitude for a fixed sonar position in the presence of volume scattering and ambient noise can be considered samples from a Rice distribution. If noise is dominant, the samples will be Rayleigh distributed. If the contribution from bottom backscatter is dominant the samples will be approximately Gaussian distributed.

If the medium between the sonar aperture and the point being interrogated is unstable in the sense that it contains spatial and temporal fluctuations in temperature and salinity, the arrival time of signals from different locations within the resolution cell will fluctuate. This can be interpreted as an uncontrolled time–varying movement and distortion of the resolution cell on the bottom. The characteristics of the variation of the measured samples will, therefore, depend on the structures within the resolution cell as well as the time scale of the variation. Further assumptions as to the contents of the resolution cell and the nature of the instabilities are necessary to describe the measured samples in terms of a probability distribution. The variation due to medium instabilities will increase with range.

6

Methods of data acquisition

An area of sea bottom can be examined by moving a sector scanning sonar along a line at constant height above the bottom. The sector scanning sonar can be mounted in two different ways. Either forward or side looking with respect to the line of translation. Each of these acquisition modes has its own advantage.

In the side looking mode range, grazing angle and bearing angle will vary for the samples corresponding to a particular position on the bottom. Due to the insensitivity of the bottom backscattering function to variations in range and grazing angle an appropriate model of the envelope amplitude is a function of bearing angle only. When noise and medium instabilities are negligible this mode of acquisition is suited for examination of the variation of bottom backscattering with bearing angle.

In the forward looking mode only range and grazing angle will vary in the middle of the sector. The bottom backscattering function corresponding to each spatial position can therefore be considered approximately constant. The variation in the samples at each spatial position will be due to noise and instabilities of the medium. This mode of acquisition is well suited to examining the bottom backscattering function when noise and instabilities of the medium are dominant. For samples acquired at angular positions off the middle of the sector the bearing angle will vary as well. Different models are therefore required for the data acquired at different positions of the sector in this mode of acquisition.

The side looking configuration is attractive as this configuration will provide information on the bottom backscattering function with bearing angle. Also, the data can be interpreted using the same model irrespective of which part of the sector was used in data acquisition. In the following the side looking mode will be examined in more detail.

7

Information extraction

The variation in envelope amplitude observed when a sidelooking sector scanning sonar is passed over a particular point on the bottom will be due to variation in the bottom backscattering function as well as noise and instabilities in the medium. The interpretation of this variation depends on the model chosen to represent the data. The primary requirement of the model is that it can accurately represent the variation in the data but also practical considerations such as processing load, memory requirements and communication of the extracted information to an operator are of importance in the selection.

If the variation of the envelope amplitude is modelled as a single stationary random process the result will be a complicated, possibly multimodal probability distribution with a large variance. The model is simple but unable to represent systematic variation in the data. Another approach is to use a nonstationary model to represent variation in envelope amplitude with bearing angle. This could describe the variation in the data but is not simple. A compromise between the stationary and non stationary models is a piecewise stationary random process within intervals of bearing angle. This approach, which is adopted here, is both simple and capable of describing a systematic variation of the envelope amplitude with bearing angle.

A procedure for data acquisition and information extraction based on a piecewise stationary model can be outlined as follows. The sector scanning sonar is moved in a side looking configuration during data acquisition. The data from each transmission is normalized, registered to a ground fixed coordinate system and interpolated into a sector image. The sector is divided into a number of subsectors each corresponding to a interval of bearing angle. When the sonar has passed an area of sea bottom a number of samples of the envelope amplitude in a number of subsectors will be available at each point on the ground.

The samples at a point in each subsector are assumed realizations of independent identically distributed random variables $A_1, A_2, \ldots, A_N$. In order to characterize a distribution at least as complicated as the Rice distribution two parameters are required. The two parameters selected here to represent the information on the distribution are the sample mean and the sample standard deviation. The population distribution function is assumed to have mean μ, variance σ^2 and existing moments up to fourth order. The sample mean is determined by

$$\hat{\mu} = \frac{1}{N}\sum_{n=1}^{N} A_n , \tag{14}$$

and the sample standard deviation by

$$\hat{\sigma} = \left[\frac{N\sum_{n=1}^{N} A_n^2 - \left(\sum_{n=1}^{N} A_n\right)^2}{N(N-1)}\right]^{1/2} . \tag{15}$$

The estimates will be jointly distributed with variances and covariance approximately given by [15]

$$V[\hat{\mu}] = \frac{\sigma^2}{N} , \tag{16}$$

$$V[\hat{\sigma}] = \frac{\mu_4 - \sigma^4}{4(N-1)\sigma^2} , \tag{17}$$

$$C[\hat{\mu},\hat{\sigma}] = \frac{\mu_3}{2(N-1)\sigma} . \tag{18}$$

Here μ_3 and μ_4 are the third and fourth order central moments of the population distribution. In order to compute the estimates $\hat{\mu}$ and $\hat{\sigma}$ it is only necessary to store N, $\sum A_n$ and $\sum A_n^2$ at each point. This has the advantage of reducing storage requirements.

The interpretation of a pair of values $(\hat{\mu}, \hat{\sigma})$ is illustrated in Fig. 6. A reference representing a background distribution must be established either by specifying a joint distribution and associated parameters or by determining the characteristics of the background empirically from the spatial distribution of data in a reference region. The center of the background is given by the mean values of the estimates $\hat{\mu}$ and $\hat{\sigma}$. For the purpose of illustration the background in Fig. 6 is assumed to be Rayleigh distributed. For a sufficiently large number of samples the sample mean and sample standard deviation can in general be assumed jointly normal. The ellipse represents a confidence level of a jointly normal distribution with parameters given by Eqs. 14–18. With the characteristics of the background established it can be tested whether a pair of $(\hat{\mu}, \hat{\sigma})$ belongs to the background. If the pair is located outside the region occupied by the background a further characterization of the data is possible based on the position of the pair relative to the center of the background distribution. Lines of location of the pair $(\hat{\mu}, \hat{\sigma})$ indicated for a number of important situations in Fig. 6. The line marked Rice has been drawn using Eq. 11. It describes the location of a pair $(\hat{\mu}, \hat{\sigma})$ resulting from a process typical of a strong scatterer on the background of a large number of weaker scatterers. The lines marked Rayleigh and Shadow describe processes with a Rayleigh distribution but with means different from the background. Both lines have been drawn on the basis of Eq. 10. Processes with a large variance relative to the mean are indicated with the lines marked Blinks and Glint. Blinks represent situations where a few closely spaced scatterers cause rapid changes in amplitude. Glints represent situations with isolated spikes in the amplitude such as specular reflections. The processes are uniquely described by the length and angle of a line from the center of the background region to the pair of estimates.

For each point on the sea bottom the procedure described above will generate information describing the process within each bearing angle interval. In order to communicate this information to an operator the following procedure is suggested. For each bearing angle interval a ground registered image is generated. If the estimated pair $(\hat{\mu}, \hat{\sigma})$ at a position is inside the background region the pixel in the image is assigned a grey value proportional to $\hat{\mu}$. If it is outside the pixel is assigned a color value indicating the position of the pair $(\hat{\mu}, \hat{\sigma})$ in the diagram in Fig. 6. This procedure will generate a number of images equal to the number of bearing angle intervals that are displayed to the operator as an animated sequence.

This display technique will deemphasize areas of the sea bottom with characteristics similar to the selected background by representing these areas in grey values and displaying the sample mean which has a smaller variance than each of the samples. Areas of the sea bottom with characteristics different from the the background will be emphasized by representing these areas in color. The color of an area is an indication of the type of process at the location. In addition, changes in the process with bearing angle can be observed in an animated sequence of images corresponding to the bearing angle intervals.

8
Experiment

To demonstrate the feasibility of the technique outlined in the previous section a simple experiment was performed. An underwater scene was constructed by placing a target in the form of a concrete cylinder with a diameter of 0.5 m and a length of 1.5 m on a nominally flat featureless sandbottom. The scene was examined by moving a sonar mounted side looking past the scene at a nominal altitude of 5 m and with a range setting of 25 m. The sonar was a SEABAT 6012 from Reson System A/S operating at 455 kHz. The angular bearing −3 dB resolution is 1.5° and the range resolution is 0.05 m. The sonar data consist of the unnormalized envelope amplitude from 60 beams in a 90° sector interpolated into raster format. The sonar images were recorded with a 20 dB dynamic range setting on a S–VHS video recorder during the experiment and later digitized using a video frame grabber. The digitized images were 512 by 480 pixel with 8 bits resolution.

The digitized images were slant range corrected assuming a flat bottom and resampled in square pixels with a side length of 68 mm. The system amplitude transfer function and amplitude variation with range were unknown. In order to obtain the normalized envelope amplitude as stated by Eq. 5, assumptions as to the variation in range due to the system, propagation medium and resolution cell size are necessary. The assumption used here is that the effects are multiplicative and varying slowly with range. At any given range the standard deviation of the data was found to be approximately proportional to the mean value. An approximate normalization of the images was obtained by logarithmically transforming the data followed by a subtraction of a 24 by 24 pixel neighbourhood mean at each location. The result was exponentially transformed. The change in the statistics of the samples by subtracting a sample mean based on a large number of samples is negligible.

The image sequence was registered manually. In images where the cylinder was visible the boundary of the cylinder highlight was determined and used to estimate the centroid position of the cylinder. A linear least squares fit to the centroid position estimates was used to determine the relative position of all images in the sequence.

The 90° sector was divided into 18 bearing angle intervals of 5°. The data in all images corresponding to a bearing angle interval were used to estimate the sample mean and sample standard deviation at all ground positions where data were available. The sample mean images for two subsectors are shown on top in Fig. 7 and 8.

The target highlight and shadow are clearly seen and some random fluctuations with high sample mean at long ranges. The increased image contrast obtained when the background variance is reduced by averaging is illustrated in Fig. 9. In both images the cylinder target is seen as a highlight with shadow. The averaged image is the sample mean in a 5° subsector based on 30 samples on average at each location.

Fig. 10 shows the two dimensional histogram [16] of sample mean and sample standard deviation of the image shown on top in Fig. 7. This histogram can be compared with Fig. 6. The central region is occupied by the background. The samples with low sample mean and low sample standard deviation correspond to the target shadow and the samples with high sample mean and low sample standard deviation correspond to the target highlight. The samples with high sample mean and high sample standard deviation are due to random fluctuations in the return from featureless areas. The spatial density of these fluctuations increase with range and is attributed to incomplete normalization due to variation in signal–to–noise ratio with range. From this histogram it can be concluded that discrimination between different regions will be possible with these data.

The characteristics of the background were determined empirically by constructing the two dimensional histogram of sample mean and sample standard deviation from the data within a reference region. The estimates within the region were based on 30 samples on average. The size of the region was 51 by 51 pixels on the ground and data from all 18 bearing angle intervals were used. The region used for the background is indicated with a rectangle in the uppermost images in Fig. 7 and 8. The cell size of the histogram was chosen to be 0.25 times the sample standard deviation of the estimates. The cells were thresholded by setting all cells to zero except cells with a count greater than one. The size of the background region in the histogram was adjusted by convolving with a 3 by 3 unity mask followed by a greater than zero threshold operation. The region occupied by the background in the two dimensional histogram of sample mean and sample standard deviation is shown in Fig. 11 as the middle grey area. In addition, the colors used to code samples outside the background region are shown. A systematic variation of covariance in the histogram of the background between subsectors was noted. It was nevertheless decided to use all subsector images in defining a common background as the variation was due to the system and not to the sea bottom.

The color coded images are shown at the lower part of Fig. 7 and 8. The background is displayed as the sample mean grey values. All samples deviating from the background are displayed in color. The target highlight and shadow are clearly discriminated. The background corresponding to the same range as the background reference region is effectively suppressed. At longer ranges some random fluctuations in featureless areas are not suppressed but can be discriminated from the target highlight by a different color. Comparison of the two images shows that the target is consistently seen in both images whereas the random fluctuations are not.

The result was essentially the same for all 18 subsector images.

9

Conclusion

The traditional characterization of the sea bottom background in a sonar image by a first order statistical model is unable to describe the background completely when the bottom backscattering function varies systematically with the position of the sonar. A model capable of representing the variation in the backscattering function with sonar position will provide more information on bottom characteristics. The change in sonar position required to obtain an independent sample is smaller for changes in bearing angle than for changes in range and grazing angle. A sequence of images acquired with a side looking sector scanning sonar is therefore well suited to extracting information on the variation of the bottom characteristics with sonar position.

A first order statistical model, piecewise stationary within limited intervals of bearing angle is capable of representing much of the variation in the envelope amplitude. Within each bearing interval a point on the sea bottom can be characterized by the sample mean and sample standard deviation of the samples of the envelope amplitude. The sample mean and the sample standard deviation can be used as features to discriminate between parts of the bottom which are normal background and parts which are not. Points which cannot be considered normal background can be further characterized on the basis of the sample mean and sample standard deviation. The extracted information can be displayed to an operator as an animated image sequence.

The feasibility of the method has been tested on data from an underwater scene consisting of a cylindrical object on a flat featureless sand bottom. The results demonstrate the improvement in image contrast obtainable by displaying the sample mean. The data allowed clear discrimination of an object from the background. The discrimination was consistently successful in all bearing angle intervals. The difficulty in performing a system–independent measurement of sea–bottom characteristics has also been demonstrated.

By providing the operator with a higher image contrast and information on the variation of backscattering characteristics of the scene with observation point, the ability of a sonar system to discriminate between objects and background will be improved.

10
Acknowledgements

I thank the following persons for their contribution to this work. The experiment was coordinated by P. Guerrini. Experimental equipment was designed by V. Manzotti. The experiment was performed on the "R/V Manning" with the assistance of A. Spairani, G. Bertoli, G. Ciuffardi, M. Paoli and M. Vittozzi. Digitization and preprocessing of the data was done by W. Zimmer and M. Cassola. I. Kirsteins and P. Gerstoft provided helpful suggestions.

References

[1] Faure, P. Theoretical Model of Reverberation Noise. Journal of the Acoustical Society of America, 36, 1964: 256–259.

[2] Middleton, D. A statistical theory of Reverberations and Similar First-Order Scattered Fields. Part I: Waveforms and the General Process. IEEE Transactions on Information Theory, vol. 13, 1967: 372-392.

[3] Ol'shevskii, V.V. Statistical Methods of Sonar. Consultants Bureau, New York, 1978.

[4] Wilson, G.R. and Powell, D.R. Probability estimates of surface and bottom reverberation. Journal of the Acoustical Society of America, 73, 1983: 195–200.

[5] Chotiros, N.P., Boehme, H., Goldsberry, T.G., Pitt, S.P., Lamb, R.A., Garcia, A.L., and Altenburg, R.A. Acoustic backscattering at low grazing angles from the ocean bottom. Part II. Statistical characteristics of bottom backscatter at a shallow water site. Journal of the Acoustical Society of America, 77, 1985: 975–982.

[6] Boehme, H. and Chotiros, N.P. Acoustic backscattering at low grazing angles from the ocean bottom. Journal of the Acoustical Society of America, 84, 1988: 1018–1029.

[7] Gensane, M. A Statistical Study of Acoustic Signals Backscattered from the Sea Bottom. IEEE Journal of Oceanic Engineering, 14, 1989: 84–93.

[8] Stanic, S. and Kennedy, E.G. Reverberation Fluctuations from a Smooth Seafloor. IEEE Journal of Oceanic Engineering, 18, 1993: 95–99.

[9] Jakeman, E. and Tough, R.J.A Non-Gaussian models for the statistics of scattered waves. Advances in Physics, Vol. 37, No. 5, 1988: 471–529.

[10] Goldstein, G.B. False-Alarm Regulation in Log-Normal and Weibull Clutter. IEEE Transactions on Aerospace and Electronic Systems, vol. 9, 1973: 85–92.

[11] Rice, S.O. Mathematical Analysis of Random Noise. In: Wax, N., ed. Selected Papers on Noise and Stochastic Processes. New York, Dover, 1954.

[12] Abramowitz M. and Stegun, I.A. Handbook of Mathematical Functions. Dover, New York, 1972: Eq. 9.7.1.

[13] Jao J.K. and Elbaum, M. First-Order Statistics of a Non-Rayleigh Fading Signal and its Detection. Proceedings of the IEEE, Vol. 66, 1978: 781–789.

[14] Nicholson, J.W. and Jaffe, J.S. Side Scan Sonar Acoustic Variability. OCEANS '88 Proceedings, 1988: 338–343.

[15] Kendall, M. and Stuart, A. The Advanced Theory of Statistics. Vol. 1, Charles Griffin & Co, London, 1977: 243–248.

[16] Niblack, W. An Introduction to Digital Image Processing. Strandberg Publishing Company, Denmark,1985: 19.

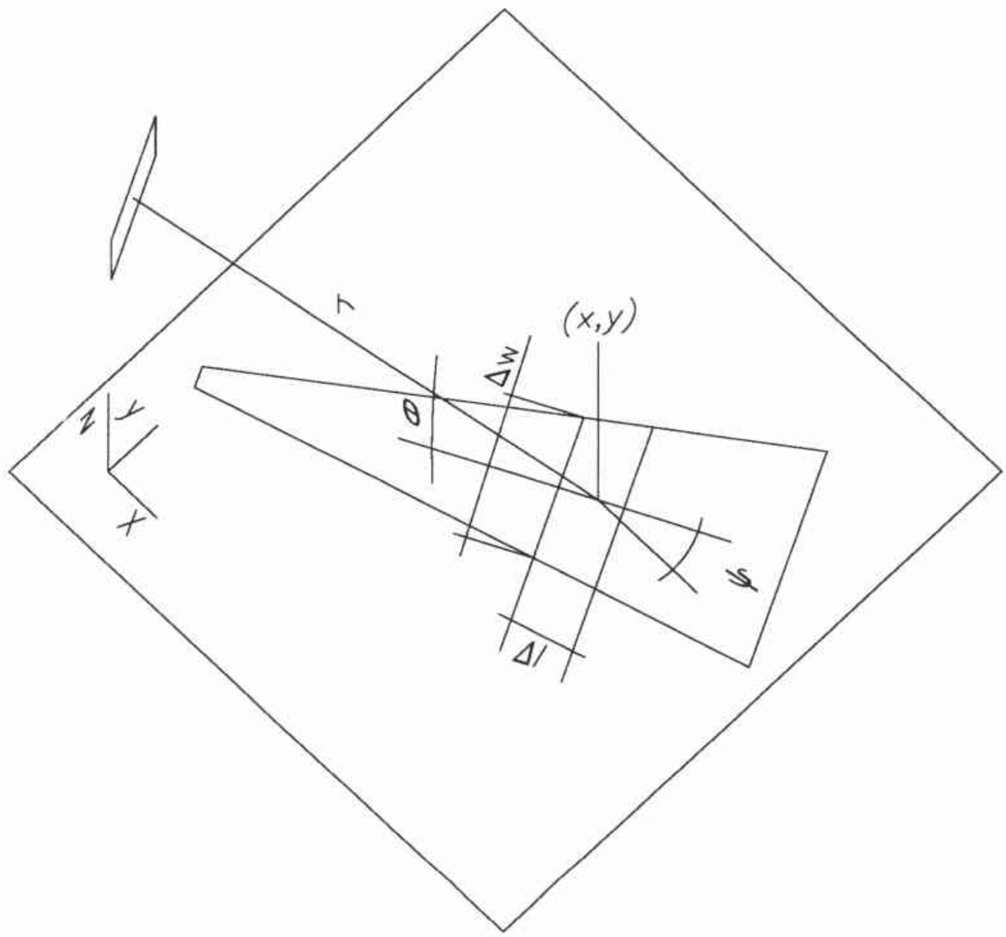

Figure 1: Geometry of experiment.

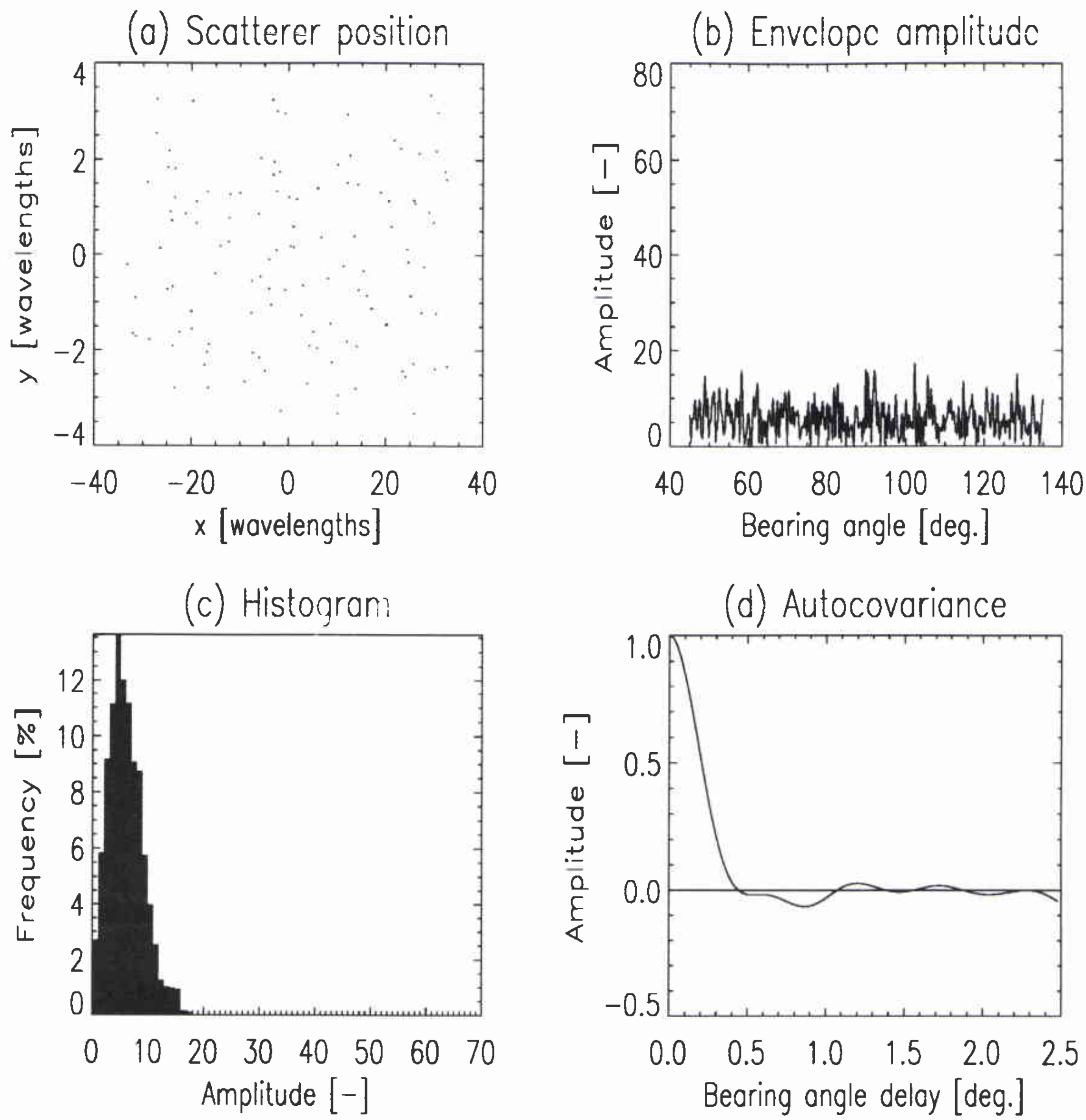

Figure 2: Background of uniformly distributed scatterers.

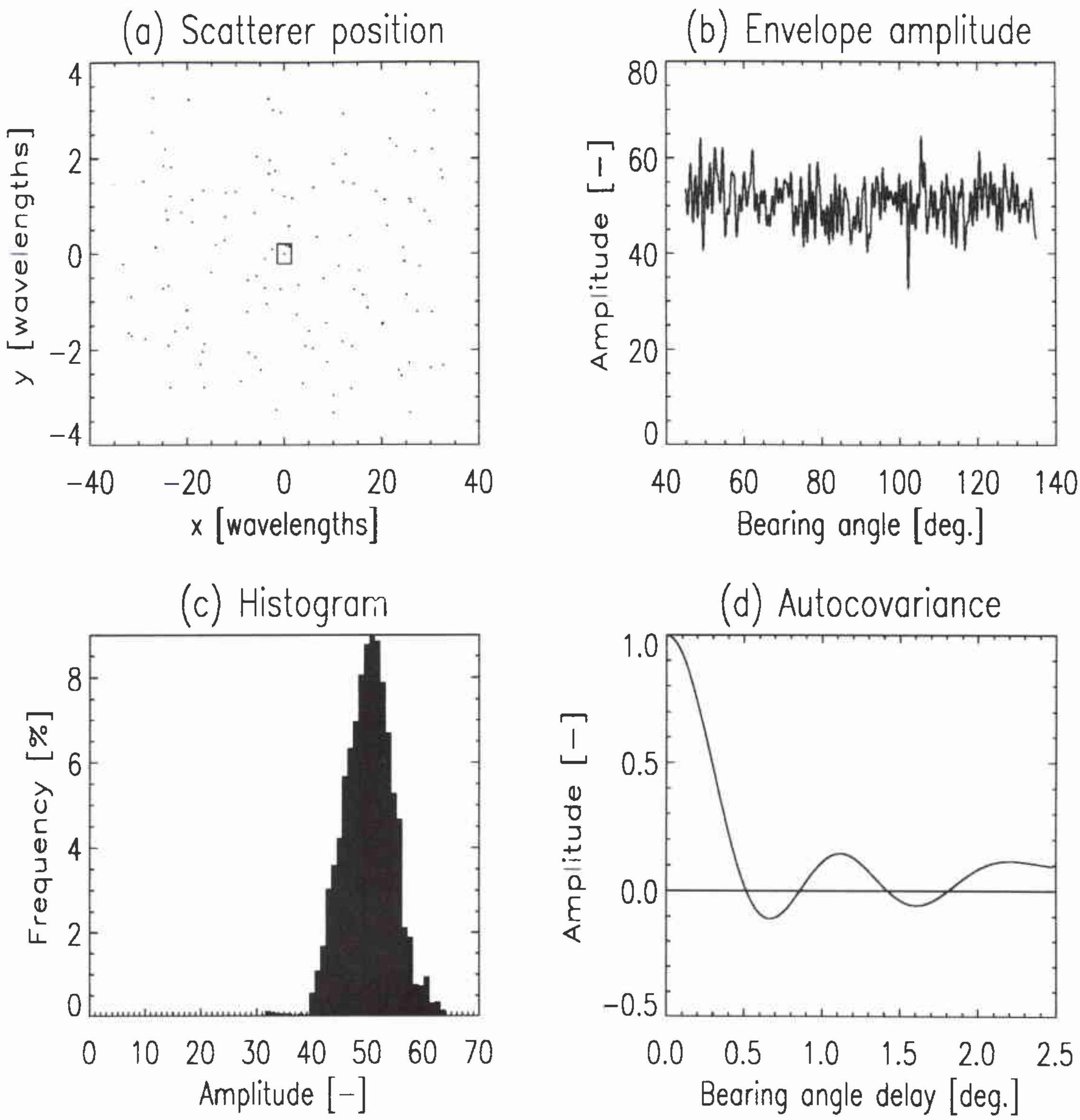

Figure 3: Background and one strong scatterer.

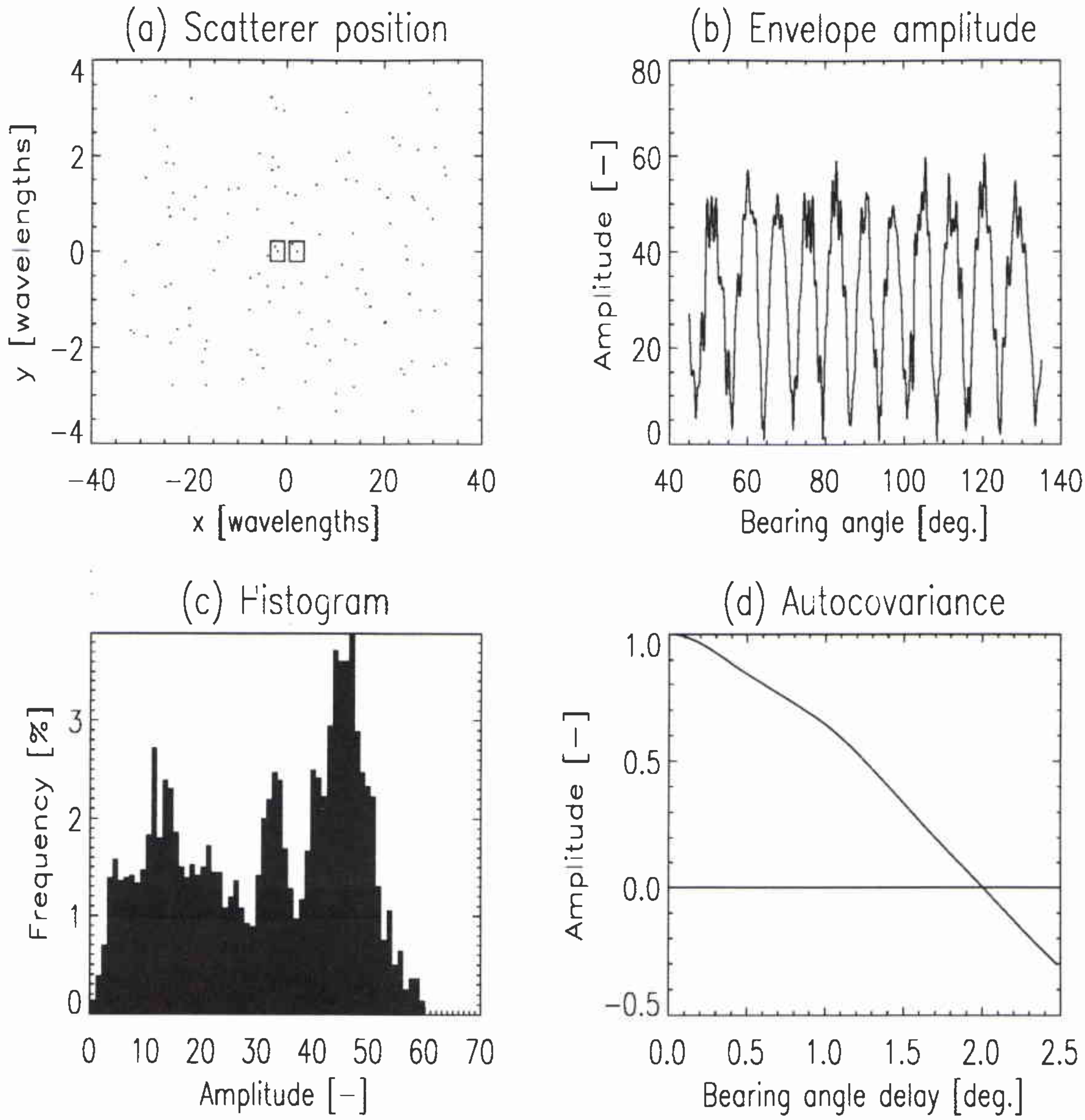

Figure 4: Background and two strong scatterers.

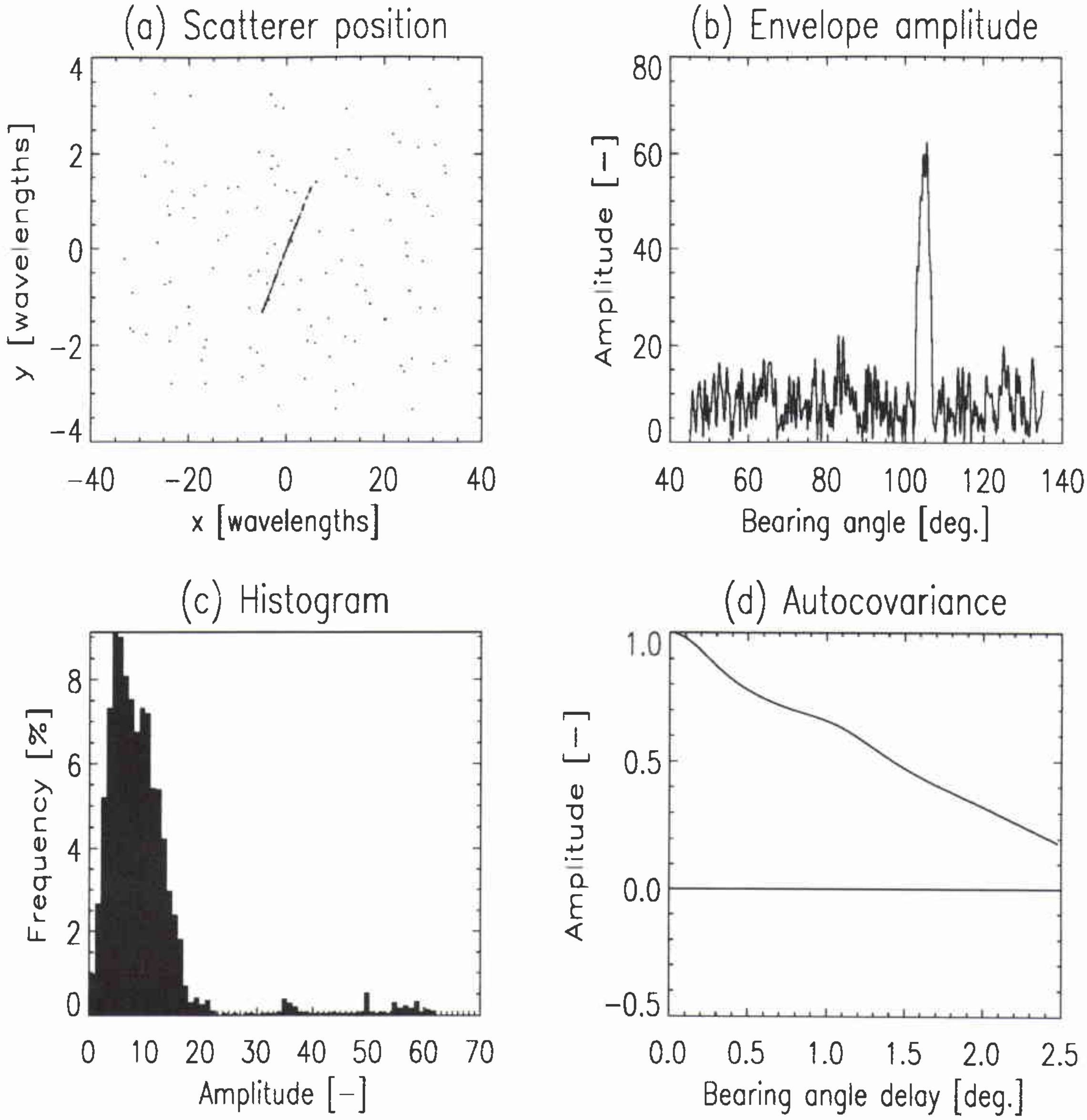

Figure 5: Background and scatterers along line.

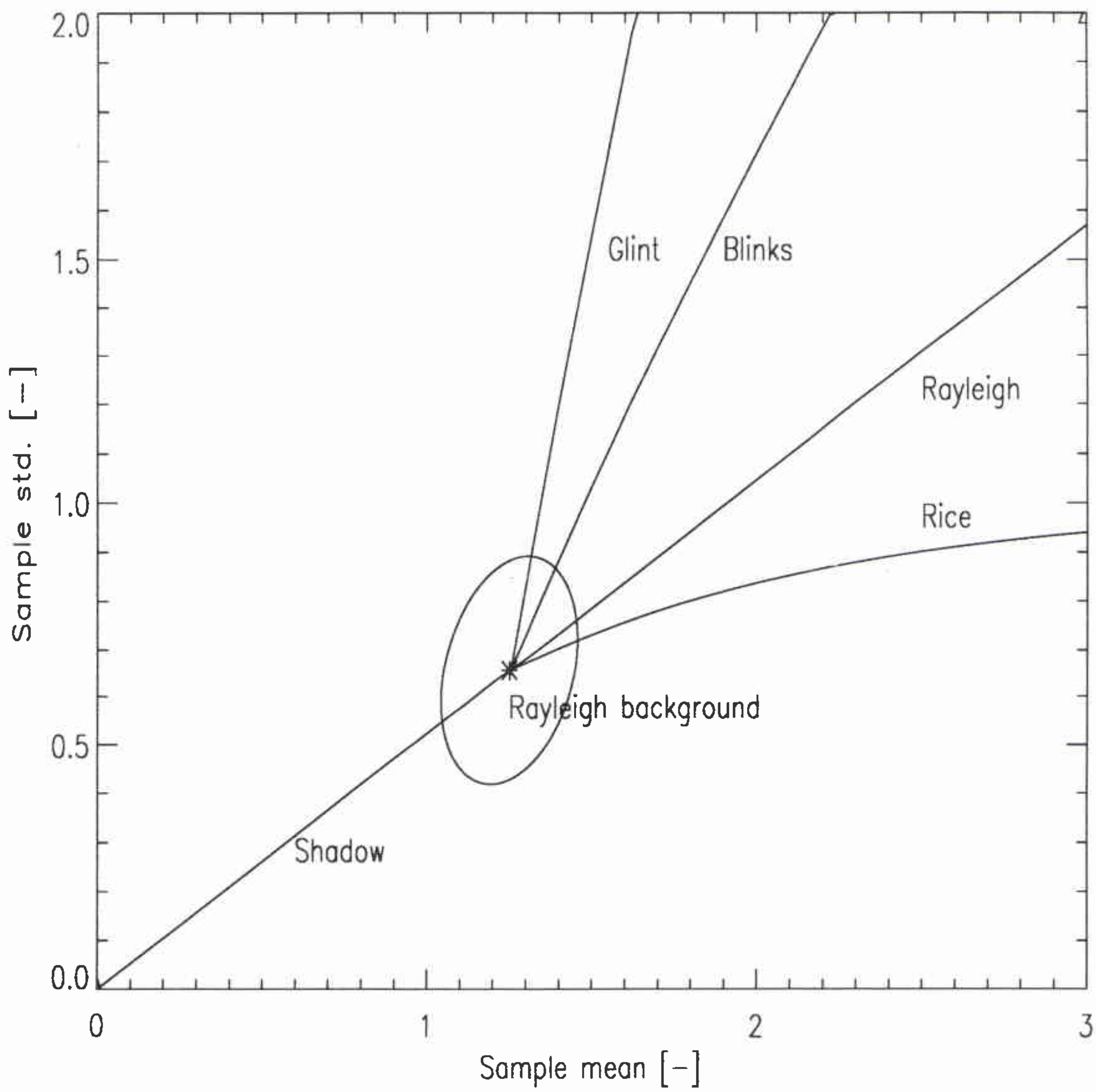

Figure 6: Interpretation of the location of mean and standard deviation estimates.

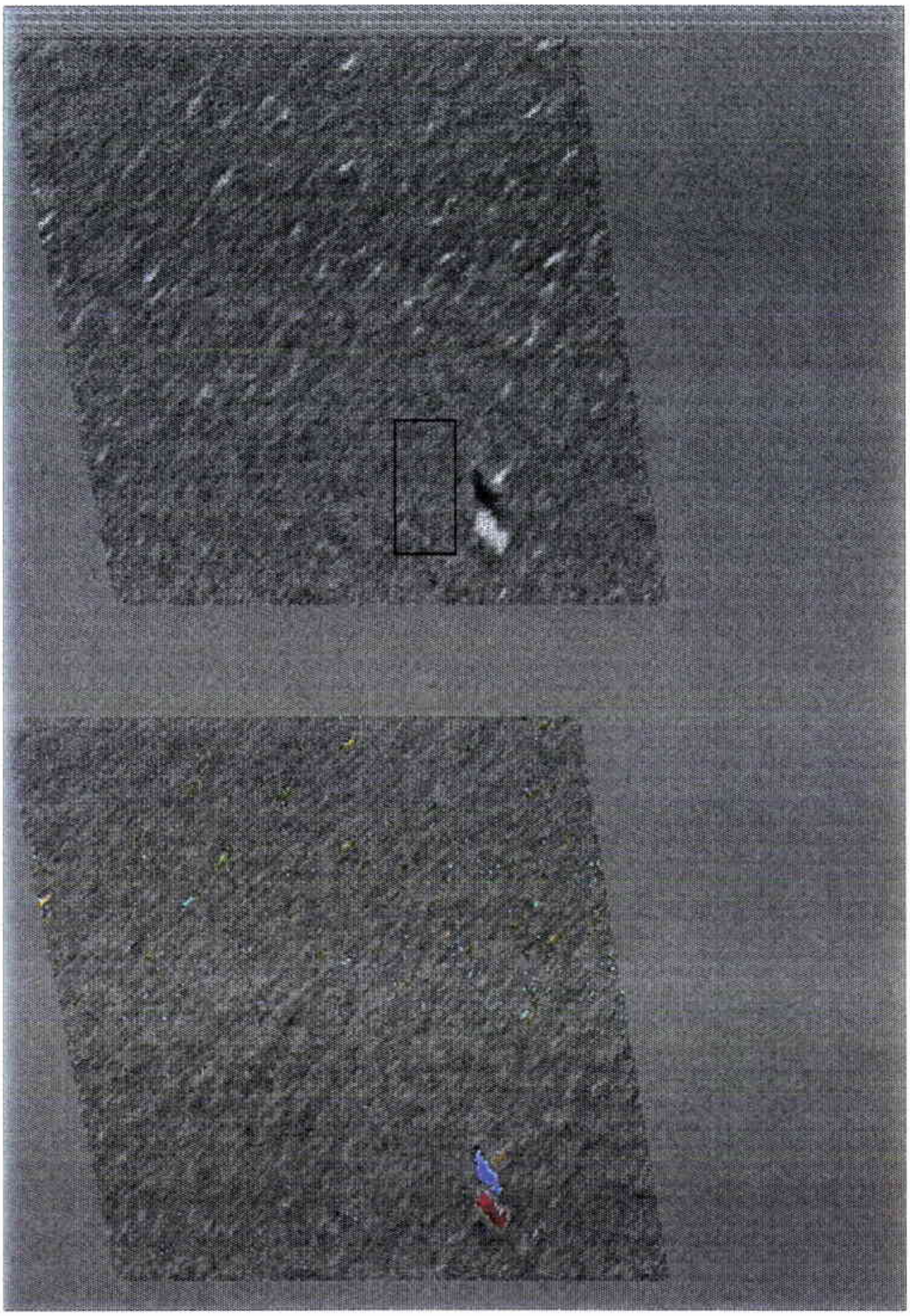

Figure 7: Bearing angle interval 4. Top: Sample mean image. Bottom: Color coded image.

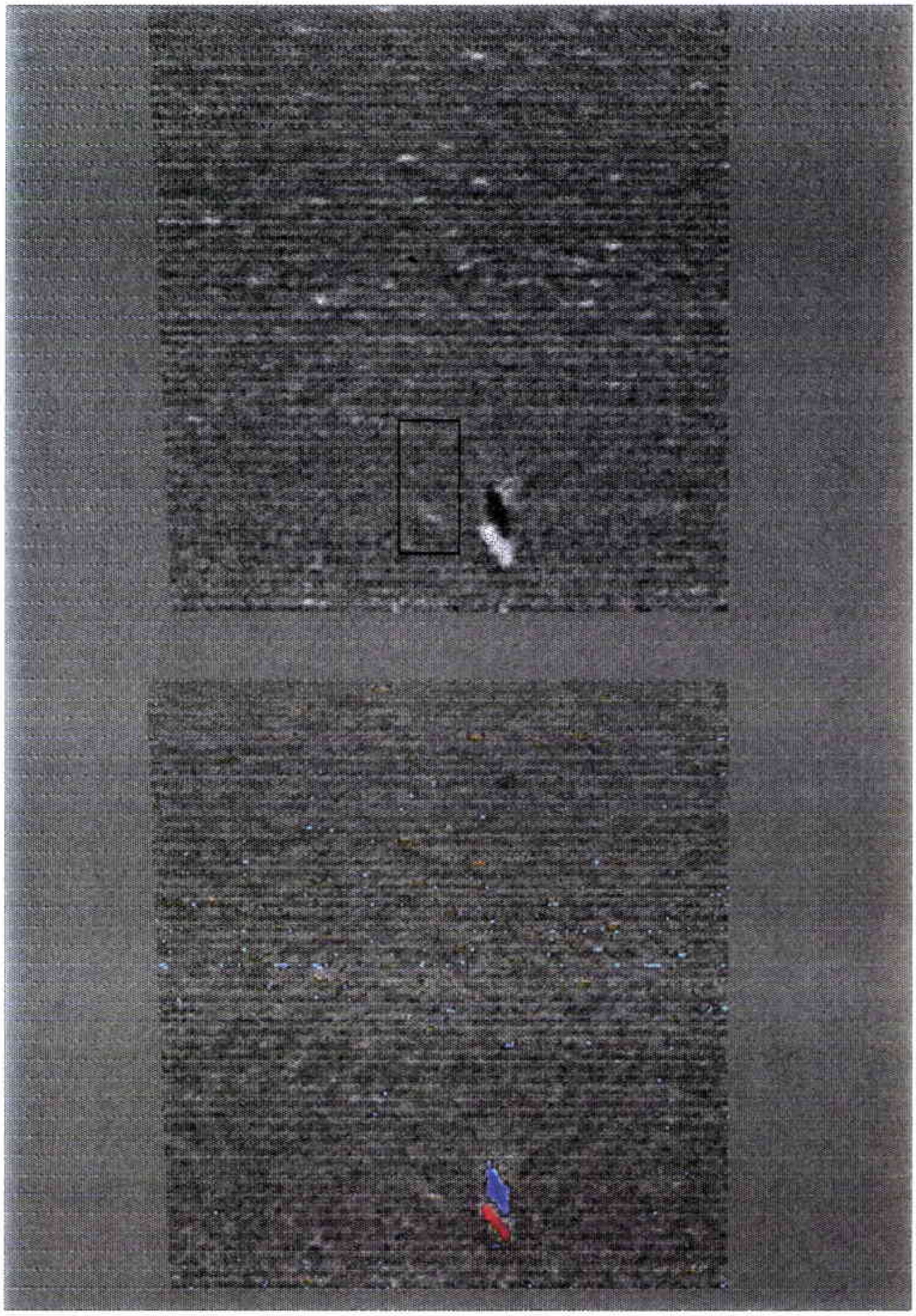

Figure 8: Bearing angle interval 8. Top: Sample mean image. Bottom: Color coded image.

intentionally blank page

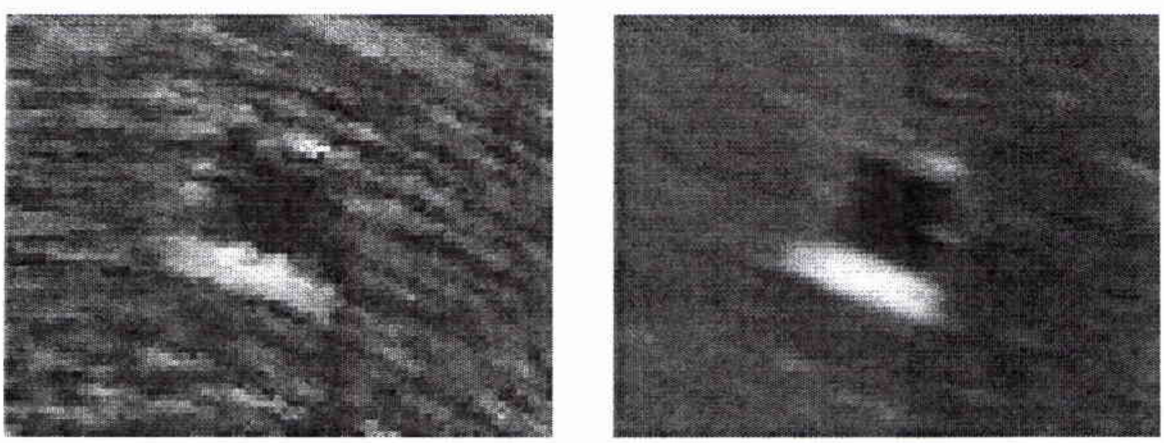

Figure 9: Comparison of raw image and image of sample mean.

intentionally blank page

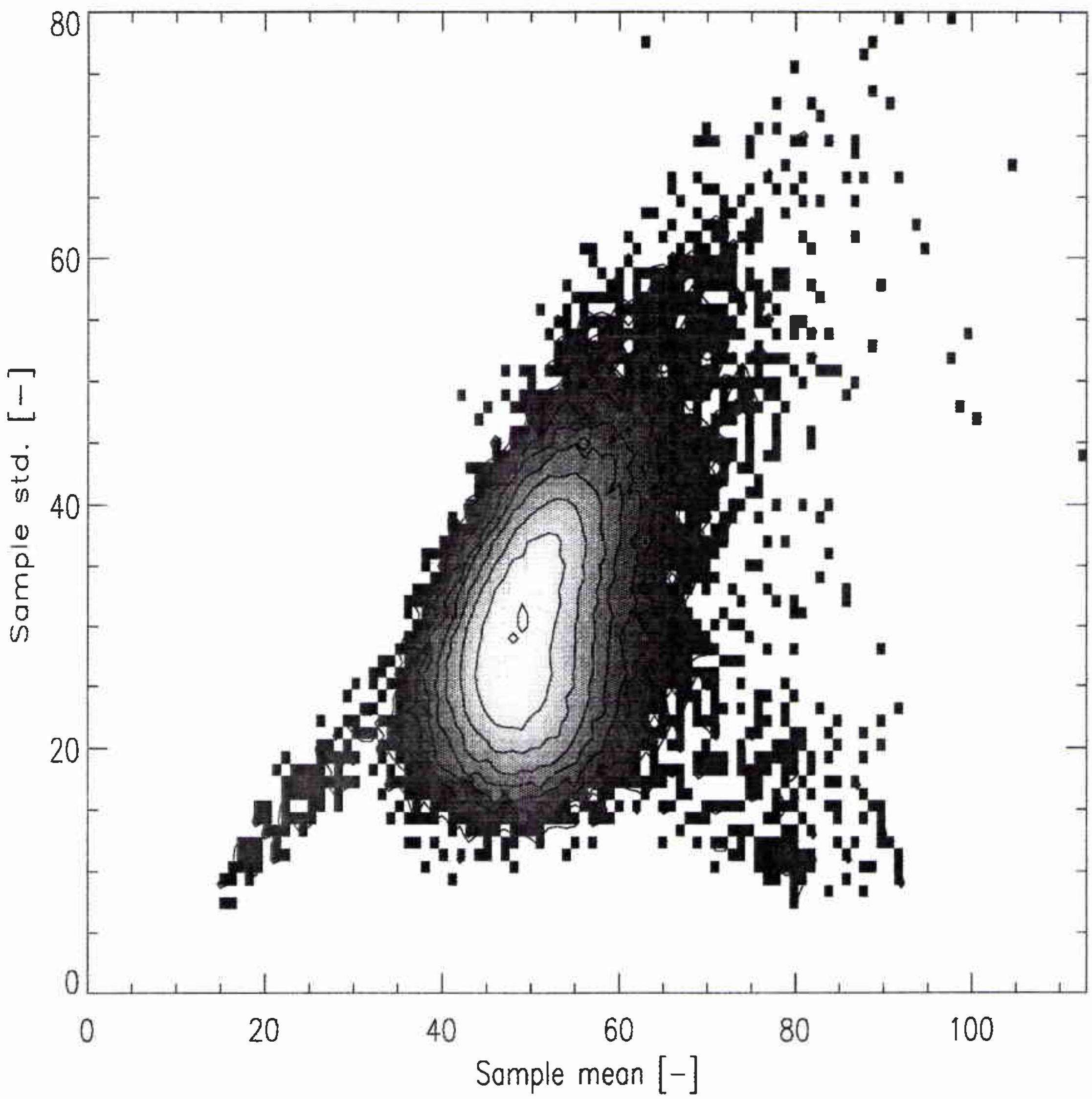

Figure 10: Two dimensional histogram of sample mean and sample standard deviation.

intentionally blank page

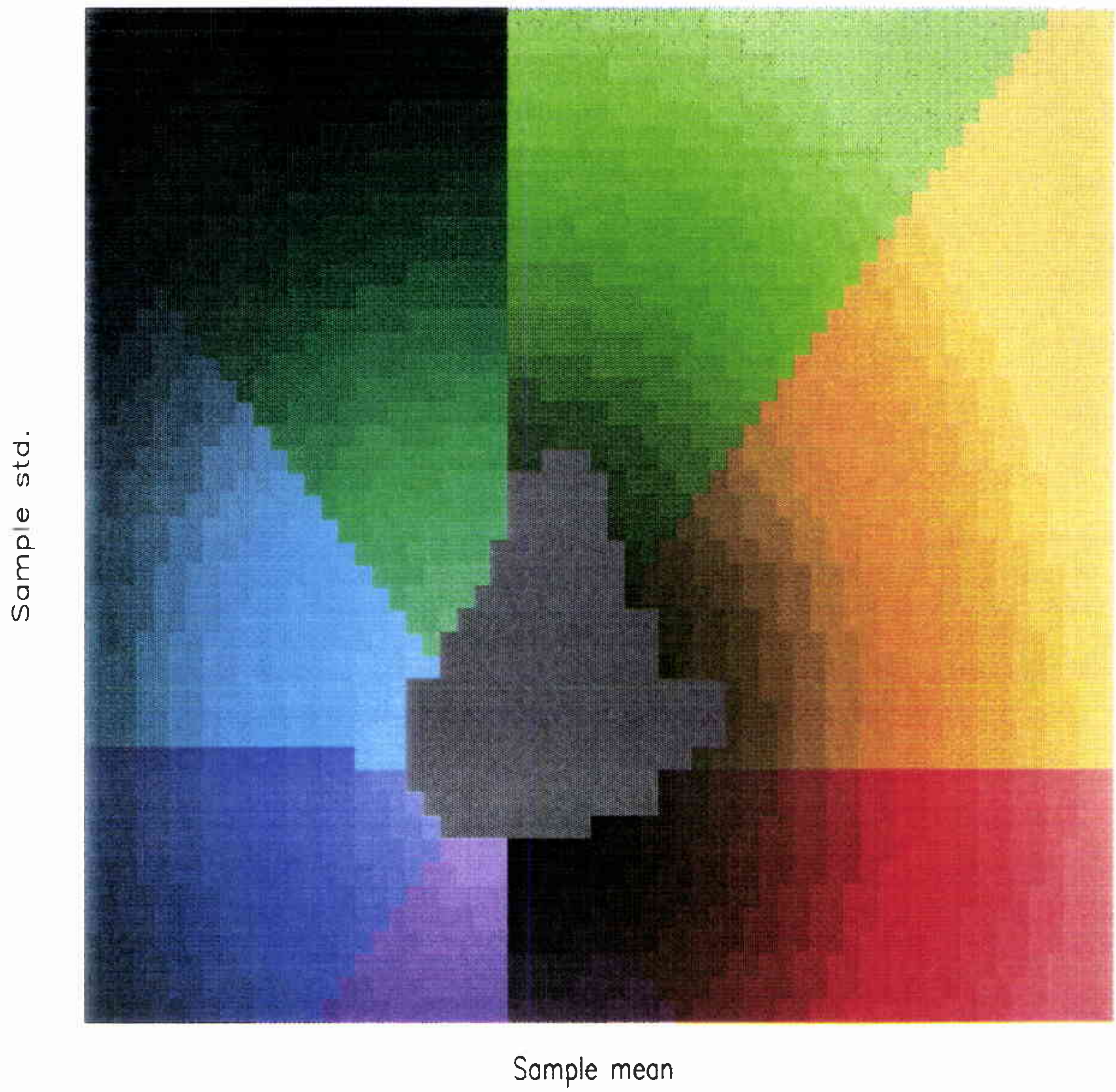

Figure 11: Two dimensional color coding scheme.

Report no. changed (Mar 2006): SM-293-UU

Document Data Sheet

NATO UNCLASSIFIED

Security Classification		Project No.
NATO UNCLASSIFIED		25
Document Serial No.	**Date of Issue**	**Total Pages**
SM-293	December 1995	41 pp.

Author(s)

B. Stage

Title

Detection of objects on a non Rayleigh background

Abstract

Sector scanning sonar systems image the sea-bottom to detect objects that can be distinguished from the background structure of the sea-bottom. In current systems images are displayed and discarded as new image data become available. In this report a method for improving sonar detection by utilizing all images in a sequence is investigated. The proposed method requires that sonar data are acquired with a sector scanning sonar in a side-looking configuration. It is demonstrated that these data can be used to detect observation point dependent changes in sea-bottom backscattering characteristics. These changes provide additional cues for discrimination that can improve the detection of objects on the sea-bottom. Results of applying the method to experimental data are presented.

Keywords

Backscattering – detection – observation point

Issuing Organization

North Atlantic Treaty Organization
SACLANT Undersea Research Centre
Viale San Bartolomeo 400, 19138 La Spezia, Italy

[From N. America: SACLANTCEN CMR-426 (New York) APO AE 09613]

Tel: +39 (0)187 540 111
Fax:+39 (0)187 524 600

E-mail: library@saclantc.nato.int

NATO UNCLASSIFIED

Report no. changed (Mar 2006): SM-293-UU

Initial Distribution for SM-293

SCNR for SACLANTCEN		*National Liaison Officers*	
SCNR Belgium	1	NLO Canada	1
SCNR Canada	1	NLO Denmark	1
SCNR Denmark	1	NLO Germany	1
SCNR Germany	1	NLO Italy	2
SCNR Greece	2	NLO Netherlands	1
SCNR Italy	1	NLO UK	3
SCNR Netherlands	1	NLO US	4
SCNR Norway	1		
SCNR Portugal	1		
SCNR Spain	1		
SCNR Turkey	1		
SCNR UK	1		
SCNR US	2		
French Delegate	1		
SECGEN Rep. SCNR	1	Total external distribution	34
NAMILCOM Rep. SCNR	1	SACLANTCEN Library	26
SACLANT	3	Total number of copies	60